Electron Lifetime in Dye-Sensitized Solar Cells: Theory and Interpretation of Measurements

Juan Bisquert,* Francisco Fabregat-Santiago, Iván Mora-Seró, Germà Garcia-Belmonte, and Sixto Giménez

Photovoltaic and Optoelectronic Devices Group, Departament de Física, Universitat Jaume I, 12071 Castelló, Spain

Received: April 23, 2009; Revised Manuscript Received: June 30, 2009

The electron lifetime τ_n in dye-sensitized solar cells (DSC) is a central quantity to determine the recombination dynamics in the solar cell. It can be measured by several methods: impedance spectroscopy, IMVS, stepped time transients, and open-circuit voltage decays. The paper aims at a better understanding of this fundamental parameter. We summarize the main models that describe the lifetime dependence on bias voltage or carrier density, and find that there are two complementary approaches to clarify the structure of the lifetime. The first is to treat the lifetime as a product of the chemical capacitance and recombination resistance. This approach is important because the resistance largely determines steady state operation characteristics of the solar cell close to open-circuit voltage. The second approach is based on a kinetic model that describes in detail the different processes governing the decay of the carrier population in a measurement of τ_n. The lifetime is composed of a trapping factor and a free electron lifetime. Since the diffusion coefficient contains the reciprocal of the trapping factor, it is found that a product (diffusion coefficient) $\times$ (lifetime) reveals the shape of the free electron lifetime, which contains the essential information on kinetics of electron transfer at the surface as a function of the position of the Fermi level. A model based on an exponential distribution of surface states provides a good description of the voltage and temperature dependence of free electron lifetime and diffusion lengths in high performance DSCs.

1. Introduction

Considerable research efforts have been devoted to the study of mesoscopic dye-sensitized solar cells (DSC) since the seminal demonstration[1] of their feasibility as a low cost photovoltaic device. Charge generation on a DSC occurs on a molecular sensitizer grafted on a nanostructured wide bandgap semiconductor. Upon excitation of the sensitizer, fast electron transfer occurs to the electron transport material. The oxidized dye is regenerated from a hole transport material or redox electrolyte. The two transport media are interpenetrated on a fine scale, allowing for a large internal interface for carrier generation. DSC devices with ruthenium sensitizers and liquid electrolytes have achieved demonstrated efficiencies over 11% at 1 full sun, and remarkable stability has been obtained using ionic liquids. Alternative configurations of nanostructured sensitized solar cells are raising a lot of interest. Quantum dot sensitized solar cell (QDSCs) performance is increasing rapidly,[2,3] and the use of ordered semiconductor architectures such as nanotubes[4] could improve the rate of electron transport and enhance diffusion lengths in DSC.[5]

The operation of solar cells is based on the competition of two basic processes.[6] On the one hand, photoexcitation and charge separation (i.e., electron injection in TiO_2 and dye regeneration in a DSC[7,8]) creates a photocurrent, which is a flow of carriers toward the outer contacts. On the other hand, recombination is an opposite flow that internally annihilates the moving carriers.[9] Recombination normally increases with the carrier density and depends (usually in exponential function) on the bias voltage V between the outer contacts. At a certain potential, recombination flow matches the photocurrent, and this equilibrium determines the open circuit voltage V_{oc} of the solar cell.

In a DSC or QDSC, transport of separated electron and hole carriers in their respective media is intercepted by interfacial charge transfer. The understanding and material control of the kinetic barriers that impede recombination are key factors for improving the performance of these solar cells. Optical transient spectroscopies have provided important insights in back electron transfer[7] and dye regeneration dynamics.[8] However, reasonably efficient devices often contain a complex combination of materials and surface treatments. Pushing performance up requires the in situ determination of the recombination flow in working devices.

Due to the complex morphology of these devices, direct measure of the recombination current does not provide sufficient information on the underlying mechanisms, and special methods have been devised based on a small perturbation approach. The solar cell is set in determined conditions of steady state by bias voltage, illumination, temperature, etc., that remain constant in time. A small variation of a stimulus signal (harmonically modulated, or stepped in time) induces a small variation of the response signal. Here "small" has a precise meaning: the response amplitude is linear to that of the signal. By these means, the quotient of both (the "transfer function") is independent of the amplitudes, and thus is a unique property of the steady state conditions. In particular, the voltage-to-current transfer function, usually termed impedance spectroscopy (IS), has emerged as a major tool for DSC characterization.[10−16] Measurements with IS technique provide a full picture of the processes determining the operation of DSCs, and this allows for a deeper study of

* To whom correspondence should be addressed. E-mail: bisquert@fca.uji.es.

10.1021/jp9037649 CCC: $40.75
Published on Web 08/18/2009

Juan Bisquert (BSc. Physics 1985, Ph.D. Physics 1992) is professor of Applied Physics at Universitat Jaume I, Spain. His recent research activity is focused on hybrid and organic photovoltaic devices, in particular dye-sensitized solar cells.

Francisco Fabregat-Santiago (BsC 1995, Ph.D. Physics 2001) is an associate professor at Universitat Jaume I, Spain. He is an expert in electro-optical characterization of devices and particularly known by his studies on the electrical characteristics of nanocolloids, nanorods, nanotubes, dye solar cells and electrochromic materials using impedance spectroscopy.

Iván Mora-Seró (M.Sc. Physics 1997, Ph.D. Physics 2004) is a researcher at Universitat Jaume I, Spain since 2002. He has worked on crystal growth and characterization of nanostructured devices, making both experimental and theoretical research. Nowadays he is focused on the study of charge generation and separation in quantum dots and the application in QDSCs.

Germà Garcia-Belmonte received his Ph.D. degree at Universidad Nacional de Educación a Distancia, 1996. Recently he follows research in various topics within the field of organic electronics and photovoltaics as electronic mechanisms in organic lightemitting diodes and plastic and thin-film solar cells. Device physics using impedance spectroscopy (including modeling and measuring) is his main subject.

Sixto Giménez is curently Ramón y Cajal researcher at the Department of Physics of the Universitat Jaume I de Castellón. His research is mainly focused on the manufacturing and electrochemical and optoelectronic characterization of QDSC.

specific aspects, avoiding the contamination of side effects in these complex devices.

It has become popular to characterize recombination in a DSC by means of a characteristic time constant that is usually called the electron lifetime, τ_n. This can be measured by intensity modulated photovoltage spectroscopy (IMVS),[17,18] which is a voltage-to-light transfer function. The electron lifetime can also be obtained by IS[14,19] and by small amplitude step time transient decays.[20−22] A widely used V_{oc} decay method[23,24] is based on the reciprocal time derivative of the open-circuit voltage decay, normalized to the thermal voltage

$$\tau_n = -\frac{k_B T}{q}\left(\frac{dV_{oc}}{dt}\right)^{-1} \quad (1)$$

Here k_B is Boltzmann's constant, T is the temperature, and q is the elementary charge. Another important quantity that gives us insight in the recombination properties of DSCs is the recombination resistance[11,13]

$$R_{rec} = \frac{1}{A}\left(\frac{\partial j_{rec}}{\partial V}\right)^{-1} \quad (2)$$

where j_{rec} is the recombination current and A is the cell area. The dominant method to obtain R_{rec} is IS.[10−14]

Essential to good device performance is that the carrier extraction time should be shorter than the recombination time. Therefore many papers report the lifetime τ_n in comparison to the characteristic transport time τ_d, that relates to the electron diffusion coefficient, D_n, and active film thickness, L, as

$$\tau_d = \frac{L^2}{D_n} \tag{3}$$

A similar procedure is to compare the diffusion length

$$L_n = \sqrt{D_n \tau_n} \tag{4}$$

with the film thickness. Since the diffusion length is the average distance that a carrier diffuses before disppearing by recombination, $L_n > L$ indicates good collection efficiency.

It is usually thought that the electron lifetime in DSC reflects the basic kinetics of the recombination of electrons. In fact, we would ideally like to reduce the measured lifetime to a set of microscopic parameters describing a capture probability, such as the formula for bulk homogeneous semiconductors

$$\tau_n = \frac{1}{\upsilon_{th} \sigma N_t} \tag{5}$$

where υ_{th} is the thermal velocity of electrons, σ is the capture cross section and N_t is the density of recombination states. However, in hybrid solar cells made of a mixture of nanoscale phases, as in semiconductors containing numerous defect levels,[25] the situation is generally quite complex. In fact τ_n may represent a combination of processes that depend not only on charge transfer kinetics but on several of the cell constituents.

Despite hundreds of measurements of τ_n having been reported in DSCs, our general understanding of the physical meaning must be rated as limited, as this is connected to the complexity of recombination in DSC. The standard redox carrier in DSC is iodine/iodide. The overall recombination reaction

$$I_3^- + 2e^-(TiO_2) \rightarrow 3I^- \tag{6}$$

consists of a multiple-step mechanism, very probably involving the species I_2,[9] and one of the steps will be rate determining. The oxidized species in the electrolyte may therefore be I_2, and/or I_3^-, and essential aspects of electron transfer are not yet known in detail.[26]

Aiming at progress toward a microscopic understanding of recombination by charge transfer in DSC devices, in this paper we try to clarify the structure of the electron lifetime in DSC. Our main strategy is to outline a general model for τ_n that contains all of the main factors that intervene in the measurement of τ_n. We also suggest to discern in the lifetime the two components that can be separately measured by IS: a resistance and a capacitance. And we take an additional step which is to identity the voltage dependence of a newly defined "free electron lifetime", that is directly related to the relatively small, but important, variations of the diffusion length that have been reported. We will discuss a variety of representative measurements to support the discussion.

2. Definition of the Lifetime

The basic definition of the electron lifetime is quite simple for a homogeneous system.[23] We identify a given electronic state populated with an ensemble of electrons with volume density n. If the recombination rate per unit volume is U_n, then the decay of a population is governed by the equation

$$\frac{dn}{dt} = -U_n(n) \tag{7}$$

We identify a small portion of the population much smaller than the average value, $\Delta n << \bar{n}$, and this decays by the law

$$\frac{d\Delta n}{dt} = -\left(\frac{\partial \bar{U}_n}{\partial n}\right)_{\bar{n}} \Delta n \tag{8}$$

Equation 8 is linear with Δn and provides always an exponential decay that defines a lifetime in terms of the recombination rate $U_n(n)$ as

$$\tau_n = \left(\frac{\partial \bar{U}_n}{\partial n}\right)_{\bar{n}}^{-1} \tag{9}$$

In the particular case that recombination rate is linear in electron density

$$U_n = k_r n \tag{10}$$

the lifetime is a constant $\tau_0 = k_r^{-1}$. However, in general eq 10 is not the case, and τ_n in eq 9 depends on the steady state via the carrier density. Moreover, often it is necessary to expand the kinetic eq 7 with trapping terms, in addition to the recombination rate, see eq 20 below. Therefore the general definition is

$$\tau_n = -\frac{\Delta n}{(d\Delta n/dt)} \tag{11}$$

The measurement of lifetime in a DSC basically consists of a perturbation of the Fermi level that induces the recombination by charge transfer. It means that the definition (11) applies to those measurements in which the excess carriers Δn are not extracted at the contacts. In ref 23, it was shown that all the methods mentioned in the Introduction to measure the lifetime in DSC provide the quantity in eq 11.

We mention a different approach, which is to define an apparent lifetime from eq 7 as[27]

$$\tau_{app} = -\frac{n}{(dn/dt)} = -\frac{n}{U_n(n)} \tag{12}$$

It should be emphasized that eq 12 uses total density and recombination rate instead of the small perturbation. However, when $U_n(n)$ is nonlinear eq 7 does not give a characteristic time. In fact it is well-known that nonexponential decay contains a distribution of lifetimes.[28] Thus τ_{app} in eq 12 cannot be measured in general and must be obtained after some data treatment.

Equation 12 is commonly used in silicon solar cells, but there one can separately measure at steady state the minority carrier density by the photovoltage (or by several contactless methods, such as photoconductance[29]) and the recombination rate (equal to photogeneration), so that τ_{app} can be measured under some conditions, especially at low injection levels, and theory exists to describe $U_n(n)$, even in the presence of defect levels or surface recombination.[30] This is very far from being the case in DSC. An established physical picture for $U_n(n)$ in DSC is not available (as the following discussion will show), and even interpretation

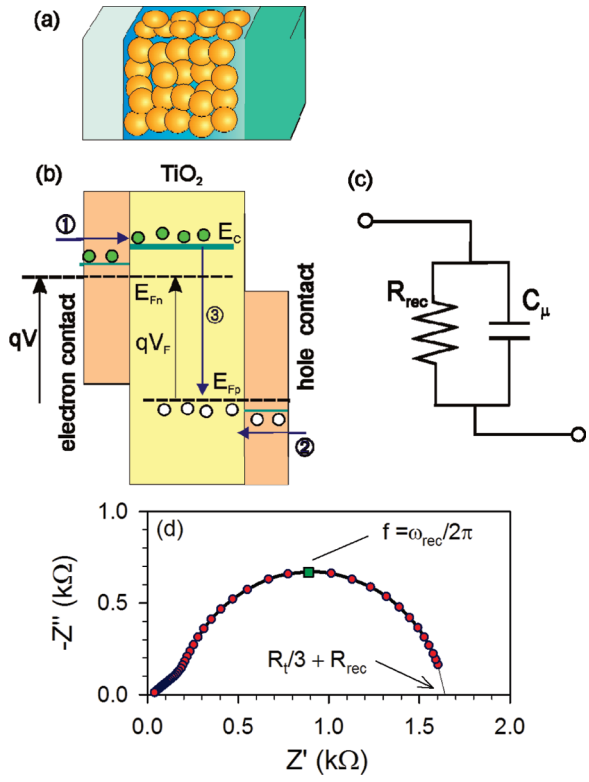

Figure 1. (a) Scheme of a DSC device. (b) Basic energy diagram indicating voltage injection of electrons (1) and holes (2) and recombination (3) processes in a DSC. Also shown are the transport energy levels and Fermi levels of electrons and holes, the potential V applied between the contacs, and the potential V_F associated with separation of Fermi levels. (c) The basic equivalent circuit for ac electrical perturbation. (d) Characteristic impedance spectra measured on a liquid electrolyte DSC showing the RC arc, and a small Warburg (diffusion) feature at high frequency.

of how n is distributed in the different kinds of electronic states is not exempt of problems. We thus restrict the discussion to quantities that can be measured in DSC. The small perturbation lifetime, that always can be measured in itself, is therefore called here simply "the lifetime", as most authors have done so far. The need to measure the small perturbation lifetime was progressively recognized in amorphous silicon[31] and crystalline silicon solar cells.[32,33]

3. Structure of the Electron Lifetime and Simple Model

A useful theoretical approach to the electron lifetime, with important practical applications as discussed later on, is to relate τ_n to equivalent circuit elements that can be separately measured by IS. As introduction to this approach we use the basic model of a solar cell described in Figure 1b, consisting on a light absorber of thickness L and area A, where the Fermi levels of electrons (E_{Fn}) and holes (E_{Fp}) are separately equilibrated to selective contacts.[6] An external bias voltage V can inject carriers and induce recombination, as shown in the figure, and correspondingly, promotion of carriers to the high energy level by photons produces a photovoltage. We point out in Figure 1b the voltage $V_F = (E_{Fn} - E_{F0})/q$ associated to the splitting of Fermi levels. In a solar cell V_F is normally less than V due to series resistances and other elements that can be identified by IS. We assume that the Fermi level of majority carrier holes, remains at dark equilibrium level, $E_{Fp} = E_{F0}$. This is usually the case in liquid electrolyte DSC where the redox energy E_{redox} of I^-/I_3^-, is not significantly modified during operation.

It is useful to underline that the simple model of Figure 1b can describe the essential operation of crystalline Si solar cells as well as DSC. The reason is that both kinds of solar cells are predominantly controlled by the variation of a single electronic carrier, and no space-charge effects that introduce strong carrier homogeneities or large electrical fields for transport need to be considered.[10,34] Although this basic model is used as a common starting point, we will also highlight the main differences between the two types of solar cells, that are mainly related to strong energy disorder in a DSC.

It is not difficult to calculate the response of the basic model of Figure 1b in IS, and the result[35] is a parallel connection of the recombination resistance R_{rec} and the chemical capacitance C_μ as shown in Figure 1c. The lower value of C_μ, inherent in an ideal model, is the chemical capacitance of the absorber. However, in a DSC the dominant contribution to C_μ is the electron transport material, the nanostructured TiO_2 as indicated in Figure 1a.[36] The density of electrons in the conduction band relates to the voltage as

$$n_c = n_0 e^{(E_{Fn}-E_{F0})/k_B T} = n_0 e^{qV_F/k_B T} \tag{13}$$

Assuming the recombination process of electrons in the semiconductor conduction band is given by eq 10, we have that $j_{rec} = qLU_n^{cb} = qLk_r n_c$ and thus

$$R_{rec} = \frac{1}{A}\left(\frac{\partial j_{rec}}{\partial V_F}\right)^{-1} = \frac{k_B T}{ALq^2 k_r} n_c^{-1} = R_0^{cb} \exp\left[-\frac{qV_F}{k_B T}\right] \tag{14}$$

The chemical capacitance for conduction band electrons is[36]

$$C_\mu^{cb} = ALq\frac{\partial n_c}{\partial V_F} = \frac{q^2 ALn_c}{k_B T} = C_{\mu 0}^{cb} \exp\left[\frac{qV_F}{k_B T}\right] \tag{15}$$

Therefore the lifetime is

$$\tau_0 = R_{rec} C_\mu^{cb} = \frac{1}{k_r} \tag{16}$$

This characteristic time corresponds to the angular frequency at the top of the arc in Figure 1d, $\omega_{rec} = \tau_0^{-1}$ and an equivalent result is obtained from IMVS. Taking a Laplace transform of the frequency response function, it is indeed shown that such frequency corresponds to the time constant for exponential decay.[23]

Equation 16 effectively shows the separation of lifetime in two main components. The rationale for this is that R_{rec} contains both a density term, which is precisely the chemical capacitance, and a kinetic constant, so the product in eq 16 leaves only the latter.

In Figure 2 we show the data of 16% efficient monocrystalline p-type silicon solar cell where such reciprocal dependence is realized.[34] The chemical capacitance, associated to minority carrier accumulation, obtained at forward bias in excess of $V_F = 0.5$ V, and the recombination resistance, compensate to provide a nearly constant lifetime at different illumination levels, Figure 2d (data values at $V_F < 0.4$ V are discussed later on). Contactless methods to determine minority carrier lifetime have

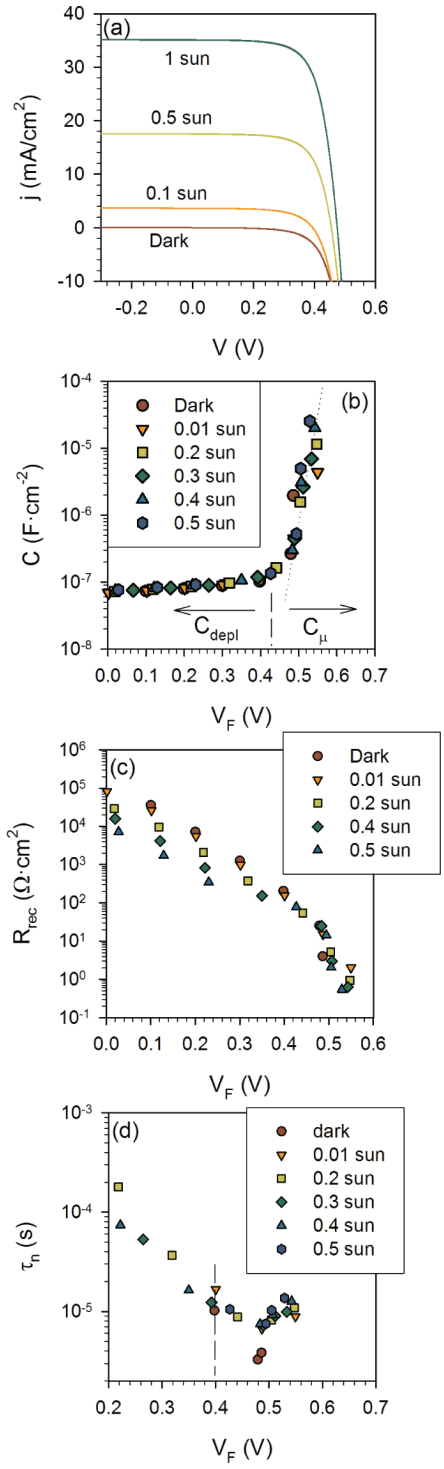

Figure 2. Experimental data for a Si monocrystalline solar cell. (a) Current density−voltage characteristic, under dark and at different illumination intensities. (b) Cell capacitance, indicating the regions of potential where the depletion layer capacitance and the chemical capacitance are separately observed. (c) Minority carrier recombination resistance. (d) Electron lifetime.

been used for many years in inorganic solar cells.[29] The results are in good agreement with the IS method.[33,37,38]

In the denominator of eq 5 we have given the microscopic expression of the kinetic rate constant, $k_r = \upsilon_{th}\sigma N_t$, in a bulk semiconductor. In a DSC, the corresponding expression is the probability of a conduction band electron to be captured by the oxidized species in the electrolyte with concentration c_{ox} (or holes, in solid DSC). On fundamental grounds, the probability

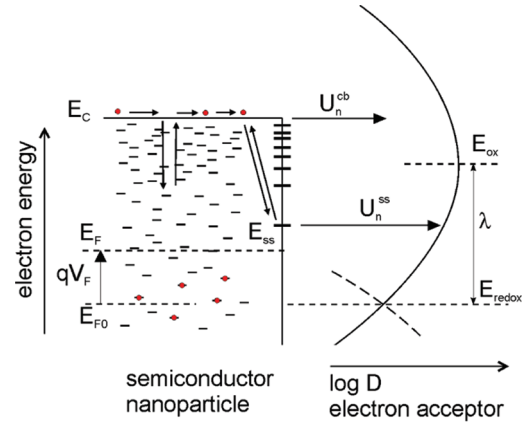

Figure 3. Schematic representation of the steps involved in the recombination between the electrons in TiO_2 nanoparticles and the oxidized species in the electrolyte (or hole conductor). E_{F0} is the position of the Fermi level in the dark, equilibrated with the redox potential E_{redox} of the acceptor species in solution, E_{Fn} is the Fermi level of electrons, and E_c is the conduction band energy. The following processes are indicated: Electron transport in the transport level; trapping and release in an exponential density of localized states in the bulk of semiconductor nanoparticles; capture and release by surface states; electron transfer through conduction band with rate U_n^{cb}; electron transfer through surface state with rate U_n^{ss}. On the right side we show the fluctuating energy levels of oxidized species in solution according to the Marcus−Gerischer model. λ is the reorganization energy of the acceptor species in the ionic or hole transport material, with an effective density of states D. E_{ox} is the most probable energy level for the oxidized state of the acceptor species.

ν_{el} of charge transfer at energy level E is given[39,40] by the Marcus model, outlined in the right-hand side of Figure 3

$$\nu_{el}(E) = 2k_0 c_{ox}\sqrt{\frac{k_B T}{4\pi\lambda}}\exp\left[-\frac{(E - E_{redox} - \lambda)^2}{4\lambda k_B T}\right] \quad (17)$$

where k_0 is a time constant for tunnelling, which is dependent on the distance of the acceptor to the surface,[41] and λ is the reorganization energy.

4. Factors Governing a Variable Lifetime in DSC

In the presence of impurity levels, lifetimes in silicon become highly variable[42−44] and even more so in amorphous inorganic semiconductors.[25] The characteristic result in DSC consists of a strong exponential decrease of τ_n with increasing carrier density or bias voltage in the solar cell, as shown in Figure 4c, and further discussed later.[18,21,24]

In order to provide a suitable framework of the interpretation of the lifetime, we consider in more detail a number of kinetic processes that are indicated in Figure 3.[24,45,46] Free (conduction band) electrons in TiO_2 nanoparticles undergo trapping-detrapping events in bandgap states. Such states can be directly measured by capacitance techniques.[47] The results usually imply an exponential distribution of localized states as described by the density of states (DOS)

$$g(E) = \frac{N_L}{k_B T_0}\exp[(E - E_c)/k_B T_0] \quad (18)$$

Here E_c is the energy of the lower edge of the conduction band, N_L is the total density, and T_0 is a parameter with

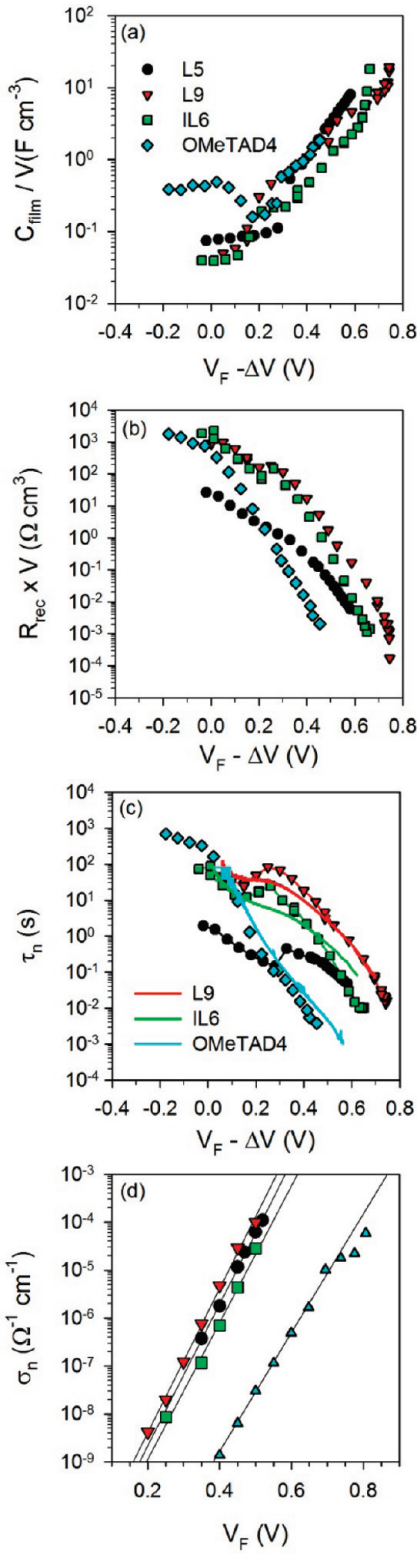

Figure 4. Parameters result from IS in the dark, as a function of potential, in several DSCs, with the following characteristics: L5: 4.6% efficient, dye N3, electrolyte H10; L9: 9.6% efficient, dye K19, electrolyte Z325; IL6: 6.3% efficient, dye K19, ionic liquid Z594; OMeTAD4: 4% efficient, dye Z907, solid hole conductor, see Table 1. (a) Chemical capacitance per unit volume. (b) Recombination resistance per volume. (c) Electron lifetime obtained from IS data (points) and V_{oc} decays (lines). (d) Electron conductivity. For comparing the results of the different samples, the values of potentials are referred to the same distance between E_{Fn} and E_C. Using the electron conductivity, L9 is taken as reference sample to determine the shifts of voltage obtaining: $\Delta V_{L5} = 20$ mV, $\Delta V_{IL6} = 39$ mV, and $\Delta V_{OMeTAD4} = 226$ mV.

temperature units that determines the depth of the distribution, which can also be expressed as a coefficient $\alpha = T/T_0$. The measured chemical capacitance is given by

$$C_\mu^{traps} = q^2 g(E_{Fn}) = C_0^{traps} \exp[qV_F/k_B T_{0b}] \quad (19)$$

where the prefactor C_0^{traps} is independent of voltage. Most of the traps may be located in the bulk of nanoparticles.

It should be emphasized that recombination is an interfacial charge transfer event at the surface between the semiconductor and the ionic/hole carrier. Since a distance for electron tunneling should be of the order of 1 nm, which is usually much less than the typical size of nanoparticles in a DSC, it is useful to distinguish between bulk traps, with parameter T_{0b}, and surface states, with a parameter T_{0s}, including in the latter class all the electronic states that participate in charge transfer.

In any transient measurement for determination of lifetime, a change of the Fermi level implies the change of occupation of bulk traps. The kinetic eq 7 must be extended as

$$\frac{\partial n_c}{\partial t} = -U_n(n_c) - \frac{\partial n_L}{\partial t} \quad (20)$$

where the last term describes the variation of free carrier density by trapping (which causes an increase of the localized electrons with density n_L) and release processes. In eq 20, U_n groups all possible channels for recombination of free carriers by charge transfer through different interfacial levels, as outlined in Figure 3. Taking into account the transfer from conduction band and from a variety of surface states (at distinct energy levels labeled $E(i)$), we may write for the rate of recombination of electrons in the conduction band, a sum of the transference rates as follows[48]

$$U_n = U_n^{cb} + \sum_{E(i)} U_n^{ss(i)} \quad (21)$$

Equation 21 contains the assumption that the electron transference occurs independently at the surface states in different energy levels. In the case of of I^-/I_3^- redox couple it is not established that charge transfer is a one electron process,[26] and we cannot rule out that different surface channels are interdependent for reaction (6). On other hand, for solid state DSC using OMeTAD hole conductor,[14] recombination is a process involving one electron and hole, very probably through a variety of channels as in eq 21.[49] In general it is very likely

TABLE 1: Properties of the Measured Dye-Sensitized Solar Cells[a]

sample	L5	L9	L10	IL6	OMeTAD 4
n-TiO_2 layer (μm)	8.1	6.8	12	6.8	1.8
scatter layer (μm)	0	4	2	4	0
dye	N3	K19	N719	K19	Z907
electrolyte	H10	Z325	Z300	Z594	solid
area (cm^2)	0.48	0.28	0.28	0.28	0.128
porosity	70%	68%	68%	68%	68%
V_{oc} (V)	0.58	0.76	0.80	0.71	0.86
J_{sc} (mA cm^{-2})	12.3	17	17.5	14.0	9.1
FF	0.66	0.72	0.73	0.71	0.51
efficiency (%)	4.6	9.6	10	6.3	4.0

[a] Please refer to the original publication for the full names of the coded dyes and electrolytes.[13,14,62]

that, rather than a single energy level, a distribution of charge transfer states exists at the interface in DSC, and we adopt the reasonable assumption in eq 21. This approach is supported by steady state measurements,[50] and important additional implications for interpretation of experimental measurements of lifetime are discussed below.

For the calculation of the lifetime from eq 20 we deal first with the trapping term, assuming in quasistatic approximation that trapped and free electrons remain in equilibrium, so that we have[46,51]

$$\frac{\partial n_L}{\partial t} = \frac{\partial n_L}{\partial n_c}\frac{\partial n_c}{\partial t} \tag{22}$$

Inserting eq 22 in 20, we obtain for a small perturbation

$$\frac{\partial \Delta n_c}{\partial t} = -\frac{1}{\left(1 + \frac{\partial n_L}{\partial n_c}\right)}\frac{\partial U_n}{\partial n_c}\Delta n_c \tag{23}$$

Equation 23 strongly suggests that we define the lifetime of free carriers, applying eq 9, as

$$\tau_f = \left(\frac{\partial U_n}{\partial n_c}\right)^{-1} = \left(\tau_0^{-1} + \sum_{E(i)} \frac{\partial U_n^{ss(i)}}{\partial n_c}\right)^{-1} \tag{24}$$

Here, $\tau_0 = \nu_{el}(E_c)^{-1}$ is the lifetime of free electrons by direct transference through conduction band, the same as that given in eq 16. Additional terms in eq 24 correspond to the transference through the bandgap surface states as indicated in Figure 3.

From eqs 23 and 24, using the general definition of eq 11, we obtain the expression for the measured lifetime

$$\tau_n = \left(1 + \frac{\partial n_L}{\partial n_c}\right)\tau_f \tag{25}$$

In eq 25, the term in parentheses corresponds to the delay by traps at the Fermi level when we attempt to measure τ_n. More precisely, by detailed balance $\partial n_L/\partial n_c = C_\mu^{traps}/C_\mu^{cb}$ equals the quotient of detrapping and trapping rates, which is a proportion of the time an electron spends in traps with respect of the time in the conduction band. This term does not correspond to the time survival of a free electron, which is given by τ_f. In general, τ_n, measured by the methods indicated in the Introduction, should be called a response time of the recombination process, but for simplicity we may still denote τ_n the "lifetime", once the content of this quantity is properly understood. It has been long recognized that trapping levels produce a considerable delay in the response time with respect to the recombination time τ_f.[42,52] For a continuous distribution of traps, increasing the Fermi level progressively occupies deep traps, and a large variation of the response time results.[53]

There is strong evidence that the trapping factor in eq 25 actually occurs in DSC. This is because the same factor applies in the measurement of the (chemical) diffusion coefficient[46,54]

$$D_n = \left(1 + \frac{\partial n_L}{\partial n_c}\right)^{-1} D_0 \tag{26}$$

Therefore, trapping factors compensate and disappear in the diffusion length, eq 4

$$L_n = \sqrt{D_0 \tau_f} \tag{27}$$

Since the diffusion coefficient of the free electrons, D_0, is believed to be constant,[55] variation of L_n should be attributed merely to the free electron lifetime τ_f. In experiments, the electron diffusion length is found to moderately vary with electron density.[22,56−58] Such variation should be proportional to $\tau_f^{1/2}$ according to the model of eq 27. The observed variations of L_n are further discussed in section 8.

5. RC Structure of the Variable Lifetime in Standard DSC

We have pointed out in section 3 that the lifetime, τ_n, measured in liquid electrolyte DSC, is related to the RC arc of IS shown in Figure 1d. This was shown in eq 15 for a preliminary simple model with a unique electronic level, and we next discuss the structure of the lifetime quite generally, including both the bulk trapping effect and the presence of several parallel channels for transference at the surface. We first give the general expressions of the model and thereafter we suggest a specific trap distribution which allows us to describe the voltage dependence of the electron lifetime and diffusion length in DSC.

Calculation of the recombination resistance, eq 2, with the general charge transfer expression in eq 21, provides the result

$$R_{rec}^{-1} = qLA\left(\frac{\partial U_n^{cb}}{\partial n_c} + \sum_{E(i)} \frac{\partial U_n^{ss(i)}}{\partial n_c}\right)\frac{\partial n_c}{\partial V_F} \tag{28}$$

and from eqs 15 and 24 we obtain

$$\tau_f = R_{rec} C_\mu^{cb} \tag{29}$$

Note that eq 29 contains the chemical capacitance of conduction band electrons. However, as shown in Figure 4, the measured chemical capacitance is usually dominated by bulk traps, eq 19. Therefore the lifetime from IS is

$$\tau_n = R_{rec} C_\mu^{traps} \tag{30}$$

We should also point out that eq 30 underlies all of the equivalent experimental methods for the measurements of lifetime in DSC.

Combining eqs 29 and 30 we find

$$\tau_n = \frac{C_\mu^{traps}}{C_\mu^{cb}}\tau_f \tag{31}$$

This is the same result as eq 25 (provided that $\partial n_L/\partial n_c \gg 1$), showing the decomposition of τ_n in trapping and free carrier lifetime terms. As mentioned above, this approach has received ample attention in the literature,[58] due to the general emphasis on the calculation of the diffusion length. Equation 31 shows that the two approaches used in this paper to model the lifetime, the kinetic model and RC approach, give the same result.

We are interested to have access to fundamental kinetic parameters of recombination. The previous analysis shows that R_{rec} contains a capacitance, and τ_n contains trapping terms. The closest we get to the recombination microscopic parameters, using the small perturbation methods, is the free electron lifetime τ_f as defined in eq 24. This parameter usually cannot be extracted from experimental data using eq 29. But we note that eq 26 can be expressed[55]

$$D_n = \frac{C_\mu^{cb}}{C_\mu^{traps}} D_0 \tag{32}$$

Therefore, combining eqs 31 and 32, we can write

$$\tau_f = \frac{D_n \tau_n}{D_0} \tag{33}$$

We can thus obtain the free electron lifetime as the product of experimental quantities: the diffusion coefficient and the measured lifetime. The denominator of eq 33 is a constant which is estimated as $D_0 = 0.4\ cm^2\ s^{-1}$.[59] It has long been recognized that the mobility-lifetime product relates to free carrier recombination time in amorphous silicon solar cells.[60,61]

6. Characteristic Experimental Results for DSC and Preliminary Interpretation

Let us discuss the characteristic experimental behavior of τ_n and R_{rec} in DSCs. Data sets representative of a variety of DSCs with different types of electrolytes and hole conductor (including two cells with volatile electrolyte with high and lower efficiency, one with ionic liquid and another one with the solid hole conductor OMeTAD) are shown in Figure 4 (Table 1).[13,14,62]

First of all we remark the exponential decrease of τ_n on bias voltage, as observed in Figure 4c, which is a characteristic result that is very well established and routinely reported in papers.[40,58,63] Furthermore good agreement is often found between the values of electron lifetime determined by independent methods.[63,64] This is confirmed in Figure 4c, that shows great coherence of the results obtained by IS and V_{oc} decays. The consistency of the outcome of different techniques clearly indicates that τ_n is an experimentally well-defined quantity that calls for a more complete understanding, since it contains important information on recombination at steady state.

In general in DSCs with a resonable performance, the photocurrent is basically determined by the absorption and injection properties of the dye and other light management aspects of the solar cell. Near the maximum power point and close to open-circuit conditions, is where the electron dynamics properties of the device have a more acute influence, via the recombination resistance, as mentioned before, Figure 4b. Therefore a combined understanding of τ_n and R_{rec}, in the region of voltage around V_{oc}, is an important key to obtain DSC with higher voltage and fill factor. Here we must highlight that the steady state current density-potential curve of a DSC, can be entirely reconstructed from the knowledge of resistances obtained by IS (by an integration procedure), provided that short-circuit photocurrent is known.[62] The most important piece of information to construct the JV curve and investigate the performance of the solar cell is the data of recombination resistance as a function of voltage.

For an interpretation of the lifetime, leading toward the extraction of the true kinetic constants that govern recombination in a DSC, we have two basic approaches.

The first approach is given by eq 25 that states that, to a large extent, the bias variation of the lifetime in a DSC is an unavoidable consequence of the disorder in the material. The fact that there is an exponential distribution of traps in the nanostructured semiconductor, introduces an exponential dependence in τ_n, via the trapping prefactor in eq 25. Besides, the crucial parameter governing recombination by interfacial charge transfer, τ_f, may also show a potential dependence on its own, as we explain in detail below.

At this point it is useful to revise the comparably simpler results obtained in the silicion solar cell, shown in Figure 2. The main difference between Figure 2 and Figure 3 is the slope of the chemical capacitances. For the silicon solar cell the slope is q/k_BT, which indicates that electron density increase is due to carriers in the conduction band. For the DSC, Figure 3a, the slope is much less steep, it is q/k_BT_0, or equivalently $\alpha q/k_BT$, indicating that the charging with electrons occurs in the exponential distribution of bandgap states. So for the silicon solar cell, the recombination resistance is given by $R_{rec} = (C_\mu^{cb})^{-1}\tau_0$ and the product $R_{rec}C$ provides a constant lifetime.

This analysis leads us to the second approach to discern the properties of τ_n in a DSC, which is via eq 30. We have already noted the slope of the traps capacitance, C_μ^{traps}, observed in Figure 4a. As for the recombination resistance, it also shows an exponential dependence of the form

$$R_{rec} = R_0' \exp\left[-\beta \frac{qV_F}{k_BT}\right] \tag{34}$$

Since the β parameter is typically in the range 0.5−0.7, we must conclude that recombination flux in a DSC cannot be simply proportional to the free electron density, which is the case described above in eq 14, and a more complex process is involved. A specific model based on eq 28 will be described later on.

We should remark in passing that eq 34 is an empirical approximation that works well in restricted domains of bias voltage. The observed dependence of recombination resistance on bias may contain additional features, such as a curvature, and also a valley, i.e., a minimum of resistance, at low potential,[65] as discussed later.

In any case, it clearly appears that in the DSC the two quantities in the product $R_{rec}C$, depart from the ideal behavior described in eqs 14 and 15. These quantities have different slopes on voltage, that are determined by constants α and β. As a consequence, and in contrast to the crystalline silicon solar cells, the lifetime τ_n in the DSC is not a constant and obtains an exponential dependence on the bias, as shown in Figure 4c.

Such variation can be attributed to the rather different features of the DSC in comparison with the bulk crystalline semiconductor. The preparation of DSC uses low temperature chemical routes, which provides a lower grade, and more disordered, semiconductor. Further, the DSC is characterized by a hugue internal interface where the recombination by charge transfer occurs. At this point it may be useful to recall that a milestone in the development of crystalline silicon photovoltaics was, and still is, the control of the main recombination interface, which is the rear contact. In a DSC the recombination interface occupies by construction the whole active layer, and it is expedient to master the properties of charge transfer events in

the path toward higher efficiencies. It should be added that the photovoltage in a DSC can double that in Si solar cell, implying a higher driving force for recombination.

7. Lifetimes and Recombination Resistance for an Exponential Distribution of Surface States

The main method of analysis of small perturbation parameters (recombination resistance, capacitance, lifetime, diffusion length) is to observe their dependence with the voltage as in Figures 2 and 4. To calculate such dependencies from the general expressions defined previously, we assume a specific model which has two main elements, as indicated in Figure 4:[24] (1) an exponential distribution of bulk trap states, with parameter T_{0b} (and $\alpha_b = T/T_{0b}$), and (2) an exponential distribution of surface states g_{ss}, with parameter T_{0s} ($\alpha_s = T/T_{0s}$).

The reasons for distinguising bulk traps and surface states have been commented above. We have already mentioned that the chemical capacitance provides a direct measure of the DOS, but it is a spatial average in which the more abundant states will dominate. Therefore in principle C_μ^{traps} in eq 19 corresponds to bulk traps located in the interior of the metal oxide nanoparticles, and a different approach is required to determine the crucial parameter involved in interfacial charge transfer, $\alpha_s = T/T_{0s}$. However, if there is evidence that interfacial traps are more abundant, or that the distribution is the same, the model can be simplified at any stage by writing simply $\alpha_s = \alpha_b = \alpha$.

The probability of charge transfer is described by eq 17. Therefore, we have that the rate of charge transfer in an interval ΔE at energy E is given by

$$U_n^{ss(i)} = g_{ss}(E_i) f(E_i, E_{Fn}) \nu_{el}(E_i) \Delta E \tag{35}$$

where $f(E,E_{Fn})$ is the Fermi-Dirac function. The calculation of R_{rec} in eq 28 with a sum (integral) over the surface state levels is

$$R_{rec}^{ss\ -1} = qAL\left(\sum_{E(i)} g_{ss}(E_i) \frac{df(E_i, E_{Fn})}{dV_F} \nu_{el}(E_i) \Delta E\right)^{-1} \tag{36}$$

The sum (or integration) in eq 36 gives the result[13]

$$R_{rec}^{ss\ -1} = q^2 AL g_{ss}(E_{Fn}) \nu_{el}(E_{Fn}) \tag{37}$$

Equation 37 states that the reciprocal charge-transfer resistance is proportional to the product of the density of surface states at the Fermi level, and the probability of electron transfer from such states. This result occurs because the resistance is a differential quantity corresponding to the current gained by a small step of voltage. A small displacement of the Fermi level fills the surface states precisely at the Fermi level, hence the resistance detects only those states.

Rearrangement of eq 37 leads to[13]

$$R_{rec}^{ss} = R_0' \exp\left[-\left(\beta - \frac{qV_F}{4\lambda}\right)\frac{qV_F}{k_B T}\right] \tag{38}$$

with R_0' a voltage-independent prefactor and

$$\beta = \frac{1}{2} + \alpha_s = 0.5 + \frac{T}{T_{0s}} \tag{39}$$

If the bias voltage V_F is considerably less than λ/q, eq 38 simplifies to eq 34. The justification to assume an exponential distrution of surface states instead of another type of distribution, is that eq 34 is in agreement with the experimental results, as shown in Figure 4c. Therefore, by the model in eq 37 we obtain a microscopic description of the β parameter that is determined in measurements of recombination in a DSC.

In eq 39 we observe that β parameter has two different components and these can be traced to eq 37. The recombination resistance decreases exponentially with the voltage by two reasons. The first is that the density of states participating in charge transfer, g_{ss}, increases when the Fermi level raises. The second is the increase of the charge transfer probability, ν_{el}, with E_{Fn}. Eventually, ν_{el} may decrease at higher voltage, provided that Marcus inverted region is reached. In this situation eq 34 is not valid and we should use a more complete expression such as eq 38.

Importantly, the two components of the recombination resistance have a different behavior with temperature, since g_{ss} should depend very weakly on T, while ν_{el} is thermally activated as indicated in eq 17. This observation forms the basis for a method to obtain $\alpha_s = T/T_{0s}$ that is discussed later. Temperature of the DSC appears as a critical variable in order to discern the microscopic components of the recombination parameter β.

Implicit in the previous modeling of R_{rec} is the assumption that surface states are occupied according to the bulk Fermi level. In general, the occupation of surface states, which loose charge by interfacial charge transfer, can be much less than a bulk bandgap state at the same energy level.[65] However, if the transfer rate is not too large, as expected in good quality DSC, a common equilibrium can be assumed. In quantitative terms, a demarcation level can be defined, above which level surface states occupation is governed by E_{Fn}. An estimation of the demarcation level in a DSC indicates that it lies quite deep, 0.30 eV above the dark Fermi level.[48] Therefore the equilibrium assumption in the model of eq 37 is well supported.

Having obtained a complete description of the recombination resistance dependence on voltage in microsocopic terms, we now use the model to derive also the potential dependence of the different quantities that can be measured with the small perturbation methods.

Using eqs 19, 30, and 39, we obtain an expression of the potential dependence of the lifetime

$$\tau_n = R_0' C_0^{traps} \exp\left[-\gamma_n \frac{qV_F}{k_B T}\right] \tag{40}$$

where

$$\gamma_n = \beta - \alpha_b = \frac{1}{2} + \alpha_s - \alpha_b \tag{41}$$

Note that $\gamma_n = 0.5$ if $\alpha_s \approx \alpha_b$. On another hand, from eq 29, the free carrier lifetime can be stated as

$$\tau_f = R_0' C_0^{cb} \exp\left[\gamma_f \frac{qV_F}{k_B T}\right] \tag{42}$$

where

$$\gamma_f = 1 - \beta = \frac{1}{2} - \alpha_s \quad (43)$$

and from eq 27, the voltage dependence of the diffusion length is

$$L_n = B \exp\left[\frac{\gamma_f}{2}\frac{qV_F}{k_B T}\right] \quad (44)$$

8. Discussion and Applications

The fundamental problem of understanding recombination mechanisms in a DSC is the interpretation of the exponent β of recombination resistance. The model suggested above, by a combination of exponential distribution of surface states, and Marcus probabilities of transfer, explains the main observed trends in the measurement, as already discussed, and provides two additional predictions.[13] First, log $R_{rec}(V_F)$ is not perfectly straight but shows a curvature over a sufficient wide bias range, eq 37, and second, β depends on temperature as indicated in eq 39. At the present time, a quantitative confirmation of this model is not generally supported, since the data at different temperatures in high performance DSCs are scarce.[13] However, both characteristics (the curvature, and temperature dependence of β) will be probably confirmed in general.

In the results compared in Figure 4 for DSCs with different types of electrolytes and dyes, it is observed that the higher efficiency reached by some of the cells is explained by the combined effect of both a higher charge transfer resistance and the higher charge injection from the dye, as suggested by the short circuit current in Table 1. In particular the solid hole conductor OMeTAD cell displays the lowest charge transfer resistance, which reduces considerably the performance although this type of DSC attains higher photovoltage, Figure 4d.[14,66]

An interpretation of the electron lifetime in DSCs requires an understanding of the exponent γ_n in eq 40. In eq 41, we note that γ_n arises from the β exponent of charge transfer resistance and α_b for bulk traps. Equation 34 is strongly supported by recombination data,[9] and the chemical capacitance of traps is also a well established result;[47] therefore, $\gamma_n = \beta - \alpha_b$ is a reliable result.

It is also interesting is to address observed properties of the diffusion length in DSCs. We note first that the diffusion length is not a transient quantity, but a steady state parameter, and consequently can be expressed in terms of the IS resistances as $L_n = L(R_{rec}/R_t)^{1/2}$, being R_t the transport resistance.[10] Therefore, bulk traps do not intervene in the diffusion length.

According to the model, L_n is proportional to the square root of the free carrier lifetime. Diffusion length in DSC usually increases slightly at increasing bias voltage.[56,58,67] Characteristic voltage dependence of L_n both for high efficiency (10%)[13] and regular efficiency (5%)[11] DSCs with liquid electrolyte are shown in Figure 5a. A similar temperature variation of L_n has been reported recently in a 11.4% efficient DSC.[16] Since characteristic β values are about 0.7, the coefficient governing the variation of L_n, following the above theory, $(1 - \beta)/2$, is indeed very small, and this provides preliminary support of the model. In addition, according to eq 43 we have $\gamma_f = 0.5 - \alpha_s$ with $\alpha_s = T/T_{0s}$. Therefore the exact value of T_{0s} and the temperature of the solar cell become critical issues. Unfortunately T_{0s} cannot be independently determined. As mentioned before, the capacitance techniques measure T_{0b} which usually ranges between 800 and 1200 K. Nonetheless it should be remarked that near room temperature we expect that $\gamma_f = 0.5 - \alpha_s$ is positive but very close to 0, so that an increase of the temperature may invert the tendency of L_n, from increasing to decreasing with the

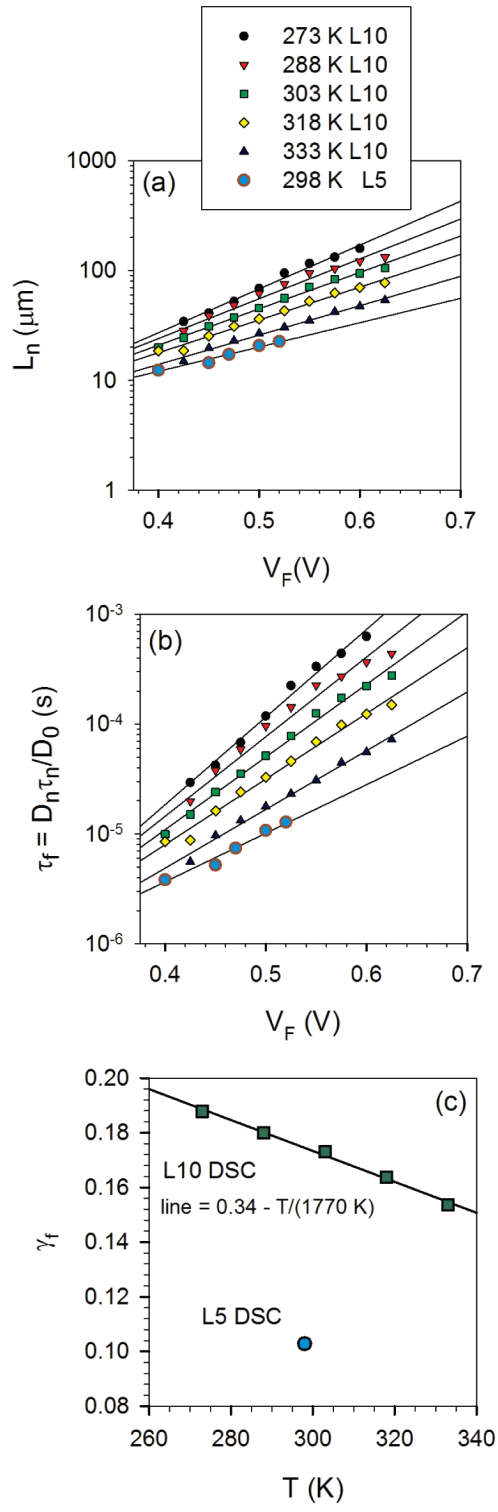

Figure 5. Parameters result from IS in the dark in several DSCs: a 10% efficient DSC (L10, dye N719, electrolyte Z300) at several temperatures and in a 4.6% efficient DSC (L5, dye N3, electrolyte H10). (a) Electron diffusion length ($L_n = \sqrt{D_n\tau_n}$) as a function of Fermi level potential. (b) The free electron lifetime τ_f, calculated from diffusion coefficient-lifetime product, indicating a best fit to a straight line that corresponds to eq 43. (c) The coefficient γ_f, defined in eq 42, as a function of temperature.

voltage. In fact for OMeTAD DSC, the diffusion length is observed to increase with voltage in the dark, while a contrary tendency is observed under illumination: it decreases with the potential,[14,59,66,68] and we may tentatively attribute this to heating of the solar cell.

Let us focus our attention on the new quantity that has been introduced above, the free carrier lifetime τ_f. As mentioned before, this is an important quantity that contains essential information on the recombination kinetics. In Figure 5b we plot the diffusion coefficient-lifetime products for the 10% and 5% efficiency DSCs as a function of voltage. From the fits to straight lines we derive the γ_f exponent that is plotted in Figure 5c. First we observe that for the 10% efficient DSC, γ_f shows a linear decrease with the temperature in good agreement with the model prediction in eq 43. A second and important result is that γ_f value decreases considerably for the less efficient solar cell, at room temperature. Using the model results we obtain that the parameter of the surface state distribution is $T_{0s} = 1770$ K for the 10% efficient DSC while it is $T_{0s} = 750$ K for the 5% efficient DSC. It means that the surface states in the more efficient DSC are much more concentrated near the conduction band edge, while in the less efficient cell the charge transfer states extend deeper in the bandgap. Therefore obtaining a large T_{0s}, which concentrates the recombination at higher voltages, could be an important reason why high performance DSC provide a large photovoltage. This interpretation illustrates the significance of the control of recombination parameters for improving the actual performance of DSCs, but must regarded as speculative until wider sets of data become available. Nonetheless we emphasize the importance of analyzing the free carrier lifetime under variation of temperature.

An important conclusion of these considerations is that exponents governing electron lifetime and free carrier lifetime variation with bias voltage, are very sensitive to temperature. Temperature has seldom been controlled in the measurements of recombination,[13,16,69] and even in these cases, it is not the ambient temperature that matters, but the internal temperature of the solar cell. In order to stabilize the measurement at illumination, DSC is irradiated during minutes or more and becomes internally heated. It may be difficult to control this problem in a device that is double glass sealed, but improvements of experimental methods are clearly necessary to progress in the understanding and control of recombination.

In the model of an exponential distribution of surface states, the recombination resistance varies continuously with the bias voltage, since more and more surface states become available for charge transfer as the Fermi level raises, eq 37. Therefore, one should recognize that the resistance in eq 34 does not provide a manifest evidence of the actual presence of the surface states. The situation is different for a monoenergetic, deep surface state.[48,50] In this case, the resistance first decreases, when the Fermi level approaches the surface state level E_{ss}, but when $E_{Fn} > E_{ss}$, the rate of trapping decreases and the resistance increases.[65] Figure 6 shows very direct evidence for charge transfer through a surface state in a QDSC with aqueous polysulfide electrolyte. The valley in R_{rec} is accompanied by a peak of the capacitance C_μ, Figure 6c, but the latter peak due to surface states is damped by the background capacitance of the exponential distribution of the bulk states, eq 19. As a result, the lifetime in Figure 6d displays a valley at low voltage that is undoubtedly associated to the surface state. This effect causes an S shape in the current−potential ($j-V$) curve as shown in Figure 6b. It is also observed that the depression in the $j-V$ curve appears at higher voltage than in the case of the lifetime.

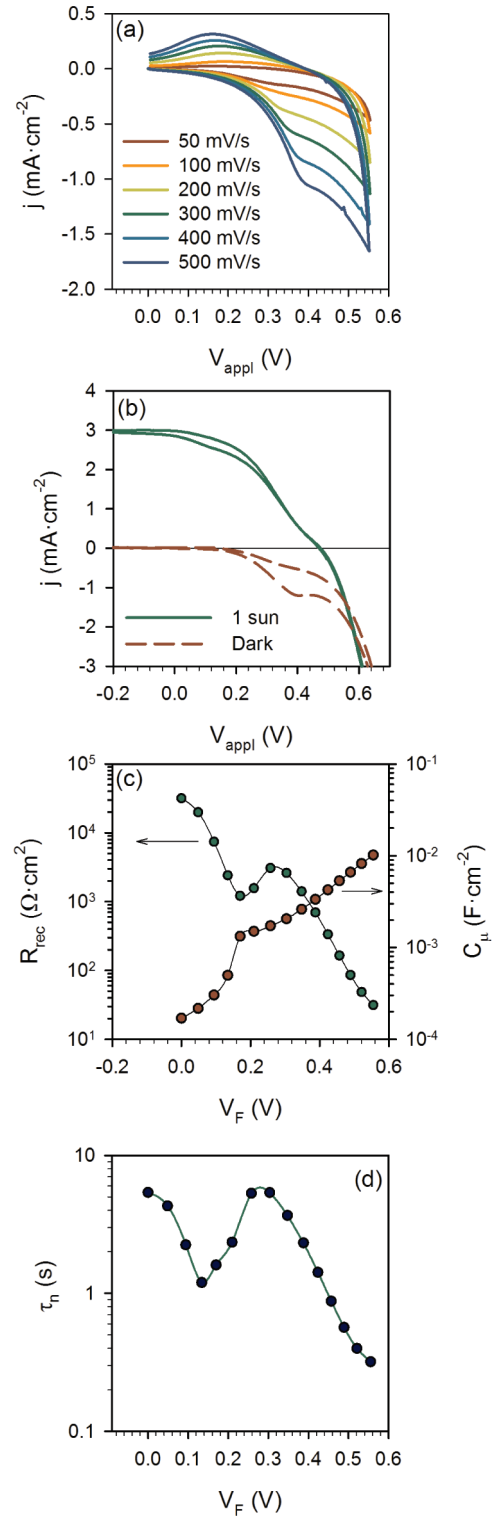

Figure 6. Experimental data of QDSC (polysulfide aqueous electrolyte) formed by mesoscopic TiO_2 sensitized with colloidal CdSe, using cysteine as a QD linker molecule, and coated with ZnS. (a) Cyclic voltammetry at different scan rates. (b) Current density−voltage characteristic, under dark and under full 1 sun illumination. (c) Charge transfer resistance and chemical capacitance. (d) Electron lifetime.

However, it must be taken into account that τ_n in Figure 6c results from a stationary measurement, while the current−potential data are obtained at a certain velocity of voltage scan. Kinetic effects progressively displace the response of the surface state to higher voltage, as shown by voltammetry data in the dark in Figure 6a.

We have argued that the response time for recombination, generally called the "lifetime", always is composed of a recombination resistance and a capacitance, and this is very directly revealed by IS measurement, as illustrated in Figure 1d. However, the time constant of the recombination arc of IS must be written, in general, as follows

$$\tau_n = R_{rec}C \quad (45)$$

Here we write C for the capacitance, which may not be chemical in origin. The nature of the capacitance is a very important issue in order to properly interpret τ_n as a lifetime. The point is very familiar in silicon solar cells. In certain conditions, the transient measurement produces a charging or discharging of the depletion layer, and then the measured "lifetime" has no relationship to recombination time at all.[70−72] This is clearly illustrated in Figure 2d: The values of τ_n at $V_F <$ 0.4 V correspond to depletion capacitance in Figure 2c and cannot be associated to the minority carrier lifetime.

This effect may be found also in some classes of nanostructured hybrid solar cells. For example it has been shown that ZnO nanowire arrays prepared by electrodeposition show a very high level of doping with a depletion region in the surface.[15,73,74] IS of DSCs prepared with such arrays will provide the impedance pattern of Figure 1d, but the time constant of the recombination arc cannot be interpreted as a recombination lifetime, since it is simply a product as indicated in eq 45, where C is a surface depletion capacitance.

Another valuable aspect of the $R-C$ approach to the electron lifetime is the control of experimental artifacts. In fact, very often the recombination arc does not singly dominate the impedance spectra, a significance portion of the capacitance may be due to counterelectrode or electrolyte diffusion contributions.[62] Time transient decays will capture such capacitances rendering the measurement of recombination time devoid of any value. While the IS measurement allows to separately recognize the recombination arc from which τ_n may be safely extracted.

It should be emphasized that in determination of electron lifetime in DSCs it is also important to check that the recombination resistance is in fact associated with interfacial charge transfer at the nanostructured metal oxide, as in some cases recombination flux is dominated by charge transfer at the exposed substrate.[75] It is generally accepted that this effect occurs at low voltage, and it can be neglected close to open-circuit voltage.

Finally, we comment briefly on the determination of carrier lifetimes in organic bulk heterojunction (BHJ) devices. Several techniques have been applied to this end,[76] including modulated photoinduced absorption,[77] transient absorption,[78] photo-CELIV,[79,80] double-injection currents,[81] and time-of-flight methods.[82] However many of these methods often depart from steady state operation of the solar cell. Some recent papers have determined the lifetime by small-amplitude perturbation of a steady state, using transient photovoltage[83] and IS.[84] In these works, it was observed that when the Fermi level of electrons increases, then (i) the lifetime decreases and (ii) the capacitance increases.[83,84] However, as generally remarked above, for a proper interpretation of the lifetime in BHJ, it is necessary to simultaneously measure the chemical capacitance, which provides access to the DOS of the electron transporting phase,[47,84] over a sufficiently wide range of variation of the Fermi level. More work in this direction is needed to clarify the interpretation of variations of the lifetime in BHJs.

9. Conclusions

The electron lifetime in dye-sensitized solar cells can be measured by several methods that usually give coherent results. We have highlighted the approach to the lifetime suggested by impedance spectroscopy, that shows that τ_n is a product of a chemical capacitance and recombination resistance. The modeling of lifetime in DSC shows two main components: a trapping factor and the free electron lifetime, τ_f. The latter quantity, τ_f, is shown to reflect the basic kinetics of recombination of free electrons, and depends on the bias when charge transfer at the metal oxide/electrolyte interface is governed by surface states. The diffusion coefficient contains the reciprocal of the trapping factor, therefore from a product $D_n\tau_n$ the potential dependence of free electron lifetime can be visualized. The temperature of the solar cell exerts an important influence on the coefficients that describe the voltage dependence of the lifetime. A model based on the transference through an exponential distribution of surface states is found to provide a good description of the observed exponential dependence of the recombination resistance with the voltage, with a parameter β. The model also accounts for the temperature variations of the free electron lifetime and electron diffusion length in high performance dye solar cells.

Acknowledgment. The work was supported by Ministerio de Ciencia e Innovación of Spain under projects HOPE CSD2007-00007 and MAT2007-62982 and Generalitat Valenciana under project PROMETEO/2009/058.

References and Notes

(1) O' Regan, B.; Grätzel, M. *Nature* **1991**, *353*, 737.
(2) Shen, Q.; Kobayashi, J.; Diguna, L. J.; Toyoda, T. *J. Appl. Phys.* **2008**, *103*, 084304.
(3) Kamat, P. V. *J. Phys. Chem. C* **2008**, *112*, 18737.
(4) Shankar, K.; Bandara, J.; Paulose, M.; Wietasch, H.; Varghese, O. K.; Mor, G. K.; LaTempa, T. J.; Thelakkat, M.; Grimes, C. A. *Nano Lett.* **2008**, *8*, 1654.
(5) Martinson, A. B. F.; Goes, M. S.; Fabregat-Santiago, F.; Bisquert, J.; Pellin, M. J.; Hupp, J. T. *J. Phys. Chem. A* 2009.
(6) Bisquert, J.; Cahen, D.; Rühle, S.; Hodes, G.; Zaban, A. *J. Phys. Chem. B* **2004**, *108*, 8106.
(7) Tachibana, Y.; Moser, J. E.; Grätzel, M.; Klug, D. R.; Durrant, J. R. *J. Phys. Chem.* **1996**, *100*, 200556.
(8) Clifford, J. N.; Palomares, E.; Nazeeruddin, M. K.; Grätzel, M.; Durrant, J. R. *J. Phys. Chem. C* **2007**, *111*, 6561.
(9) Huang, S. Y.; Schilchthörl, G.; Nozik, A. J.; Grätzel, M.; Frank, A. J. *J. Phys. Chem. B* **1997**, *101*, 2576.
(10) Bisquert, J. *J. Phys. Chem. B* **2002**, *106*, 325.
(11) Fabregat-Santiago, F.; Bisquert, J.; Garcia-Belmonte, G.; Boschloo, G.; Hagfeldt, A. *Sol. Energy Mater. Sol. Cells* **2005**, *87*, 117.
(12) Wang, Q.; Moser, J.-E.; Grätzel, M. *J. Phys. Chem. B* **2005**, *109*, 14945.
(13) Wang, Q.; Ito, S.; Grätzel, M.; Fabregat-Santiago, F.; Mora-Seró, I.; Bisquert, J.; Bessho, T.; Imai, H. *J. Phys. Chem. B* **2006**, *110*, 19406.
(14) Fabregat-Santiago, F.; Bisquert, J.; Cevey, L.; Chen, P.; Wang, M.; Zakeeruddin, S. M.; Grätzel, M. *J. Am. Chem. Soc.* **2009**, *131*, 558.
(15) He, C.; Zheng, Z.; Tang, H.; Zhao, L.; Lu, F. *J. Phys. Chem. C* **2009**, *113*, 10322.
(16) Cao, Y.; Bai, Y.; Yu, Q.; Cheng, Y.; Liu, S.; Shui, D.; Gao, F.; Wang, P. *J. Phys. Chem. C* **2009**, 113 ASAP.
(17) Schlichthörl, G.; Huang, S. Y.; Sprague, J.; Frank, A. J. *J. Phys. Chem. B* **1997**, *101*, 8141.
(18) Okermann, T.; Zhang, D.; Yoshida, T.; Minoura, H. *J. Phys. Chem. B* **2004**, *108*, 2227.
(19) Fabregat-Santiago, F.; García-Cañadas, J.; Palomares, E.; Clifford, J. N.; Haque, S. A.; Durrant, J. R.; Garcia-Belmonte, G.; Bisquert, J. *J. Appl. Phys.* **2004**, *96*, 6903.
(20) O'Regan, B. C.; Scully, S.; Mayer, A. C.; Palomares, E.; Durrant, J. R. *J. Phys. Chem. B* **2005**, *109*, 4616.
(21) Nakade, S.; Kanzaki, T.; Wada, Y.; Yanagida, S. *Langmuir* **2005**, *21*, 10803.
(22) Nissfolk, J.; Fredin, K.; Hagfeldt, A.; Boschloo, G. *J. Phys. Chem. B* **2006**, *110*, 17715.

(23) Zaban, A.; Greenshtein, M.; Bisquert, J. *ChemPhysChem* **2003**, *4*, 859.
(24) Bisquert, J.; Zaban, A.; Greenshtein, M.; Mora-Seró, I. *J. Am. Chem. Soc.* **2004**, *126*, 13550.
(25) Shen, D. S.; Conde, J. P.; Chu, V.; Wagner, S. *J. Appl. Phys.* **1994**, *75*, 7349.
(26) Peter, L. M. *J. Phys. Chem. C* **2007**, *111*, 6601.
(27) Hornbeck, J. A.; Haynes, J. R. *Phys. Rev.* **1955**, *97*, 311.
(28) Alcala, J. R.; Gratton, E.; Prendergast, F. G. *Biophys. J.* **1987**, *51*, 597.
(29) Sinton, R. A.; Cuevas, A. *Appl. Phys. Lett.* **1996**, *69*, 2510.
(30) Macdonald, D.; Kerr, M.; Cuevas, A. *Appl. Phys. Lett.* **1999**, *75*, 1571.
(31) Ritter, D.; Zeldov, E.; Weiser, K. *Phys. Rev. B* **1988**, *38*, 8296.
(32) Brendel, R. *Appl. Phys. A: Mater. Sci. Process.* **1995**, *60*, 523.
(33) Schmidt, J. *IEEE Trans. Electron Devices* **1999**, *46*, 2018.
(34) Mora-Seró, I.; Garcia-Belmonte, G.; Boix, P. P.; Vázquez, M. A.; Bisquert, J. *Energy Environ. Sci.* **2009**, *2*, 678.
(35) Mora-Seró, I.; Bisquert, J.; Fabregat-Santiago, F.; Garcia-Belmonte, G.; Zoppi, G.; Durose, K.; Proskuryakov, Y. Y.; Oja, I.; Belaidi, A.; Dittrich, T.; Tena-Zaera, R.; Katty, A.; Lévy-Clement, C.; Barrioz, V.; Irvine, S. J. C. *Nano Lett.* **2006**, *6*, 640.
(36) Bisquert, J. *Phys. Chem. Chem. Phys.* **2003**, *5*, 5360.
(37) Garcia-Belmonte, G.; García-Cañadas, J.; Mora-Seró, I.; Bisquert, J.; Voz, C.; Puigdollers, J.; Alcubilla, R. *Thin Solid Films* **2006**, *514*, 254.
(38) Mora-Seró, I.; Luo, Y.; Garcia-Belmonte, G.; Bisquert, J.; Muñoz, D.; Voz, C.; Puigdollers, J.; Alcubilla, R. *Sol. Energy Mater. Sol. Cells* **2008**, *92*, 505.
(39) Lyon, L. A.; Hupp, J. T. *J. Phys. Chem. B* **1999**, *103*, 4623.
(40) Miyashita, M.; Sunahara, K.; Nishikawa, T.; Uemura, Y.; Koumura, N.; Hara, K.; Mori, A.; Abe, T.; Suzuki, E.; Mori, S. *J. Am. Chem. Soc.* **2008**, *130*, 17874.
(41) Clifford, J. N.; Palomares, E.; Nazeeruddin, M. K.; Grätzel, M.; Nelson, J.; Li, X.; Long, N. J.; Durrant, J. R. *J. Am. Chem. Soc.* **2004**, *126*, 5225.
(42) Fan, H. Y. *Phys. Rev.* **1953**, *92*, 1424.
(43) Hornbeck, J. A.; Haynes, J. R. *Phys. Rev.* **1955**, *97*, 311.
(44) McIntosh, K. R.; Paudyal, B. B.; Macdonald, D. H. *J. Appl. Phys.* **2008**, *104*, 084503.
(45) Bisquert, J.; Garcia-Belmonte, G.; Pitarch, A. *ChemPhysChem* **2003**, *4*, 287.
(46) Bisquert, J.; Vikhrenko, V. S. *J. Phys. Chem. B* **2004**, *108*, 2313.
(47) Bisquert, J.; Fabregat-Santiago, F.; Mora-Seró, I.; Garcia-Belmonte, G.; Barea, E. M.; Palomares, E. *Inorg. Chim. Acta* **2008**, *361*, 684.
(48) Bisquert, J.; Zaban, A.; Salvador, P. *J. Phys. Chem. B* **2002**, *106*, 8774.
(49) Bisquert, J.; Palomares, E.; Qiñones, C. A. *J. Phys. Chem. B* **2006**, *110*, 11284.
(50) Salvador, P.; González-Hidalgo, M.; Zaban, A.; Bisquert, J. *J. Phys. Chem. B* **2005**, *109*, 15915.
(51) Bisquert, J. *Phys. Rev. B* **2008**, *77*, 235203.
(52) Haynes, J. R.; Hornbeck, J. A. *Phys. Rev.* **1953**, *90*, 152.
(53) Rose, A. *Concepts in Photoconductivity and Allied Problems*; Interscience: New York, 1963.
(54) Bisquert, J. *J. Phys. Chem. B* **2004**, *108*, 2323.
(55) Bisquert, J. *Phys. Chem. Chem. Phys.* **2008**, *10*, 3175.
(56) Fisher, A. C.; Peter, L. M.; Ponomarev, E. A.; Walker, A. B.; Wijayantha, K. G. U. *J. Phys. Chem. B* **2000**, *104*, 949.
(57) Krüger, J.; Plass, R.; Grätzel, M.; Cameron, P. J.; Peter, L. M. *J. Phys. Chem. B* **2003**, *107*, 7536.
(58) Peter, L. M.; Dunn, H. K. *J. Phys. Chem. C* **2009**, *113*, 4726.
(59) Jennings, J. R.; Peter, L. M. *J. Phys. Chem. C* **2007**, *111*, 16100.
(60) Street, R. A. *Appl. Phys. Lett.* **1982**, *41*, 1060.
(61) Crandall, R. S.; Balberg, I. *Appl. Phys. Lett.* **1991**, *58*, 508.
(62) Fabregat-Santiago, F.; Bisquert, J.; Palomares, E.; Otero, L.; Kuang, D.; Zakeeruddin, S. M.; Grätzel, M. *J. Phys. Chem. C* **2007**, *111*, 6550.
(63) Miettunen, K.; Halme, J.; Toivola, M.; Lund, P. *J. Phys. Chem. C* **2008**, *112*, 4011.
(64) Miettunen, K.; Halme, J.; Lund, P. *J. Phys. Chem. C* **2009**, 113 ASAP.
(65) Mora-Seró, I.; Bisquert, J. *Nano Lett.* **2003**, *3*, 945.
(66) Wang, M.; Chen, P.; Humphry-Baker, R.; Zakeeruddin, S. M.; Grätzel, M. *ChemPhysChem* **2009**, *10*, 290.
(67) Barnes, P. R. F.; Anderson, A. Y.; Koops, S.; Durrant, J. R.; O'Regan, B. *J. Phys. Chem. C* **2009**, *113*, 1126.
(68) Snaith, H. J.; Grätzel, M. *Adv. Mater.* **2007**, *19*, 3643.
(69) O'Regan, B.; Durrant, J. R. *J. Phys. Chem. B* **2006**, *110*, 8544.
(70) Castañer, L.; Vilamajo, E.; Llaberia, J.; Garrido, J. *J. Phys. D: Appl. Phys.* **1981**, *14*, 1867.
(71) Bail, M.; Schulz, M.; Brendel, R. *Appl. Phys. Lett.* **2003**, *82*, 757.
(72) Cuevas, A.; Recart, F. *J. Appl. Phys.* **2005**, *98*, 074507.
(73) Mora-Seró, I.; Fabregat-Santiago, F.; Denier, B.; Bisquert, J.; Tena-Zaera, R.; Elias, J.; Lévy-Clement, C. *Appl. Phys. Lett.* **2006**, *89*, 203117.
(74) Tena-Zaera, R.; Elias, J.; Leìvy-Cleìment, C.; Bekeny, C.; Voss, T.; Mora-Seroì, I.; Bisquert, J. *J. Phys. Chem. C* **2008**, *112*, 16318.
(75) Cameron, P. J.; Peter, L. M. *J. Phys. Chem. B* **2005**, *109*, 7392.
(76) Pivrikas, A.; Sariciftci, N. S.; Juska, G.; Österbacka, R. *Prog. Photovoltaics: Res. Appl.* **2007**, *15*, 677.
(77) Arndt, C.; Zhokhavets, U.; Mohr, M.; Gobsch, G.; Al-Ibrahim, M.; Sensfuss, S. *Synth. Met.* **2004**, *147*, 257.
(78) Shuttle, C. G.; O'Regan, B.; Ballantyne, A. M.; Nelson, J.; Bradley, D. D. C.; Durrant, J. R. *Phys. Rev. B* **2008**, *78*, 113201.
(79) Mozer, A. J.; Dennler, G.; Sariciftci, N. S.; Westerling, M.; Pivrikas, A.; Österbacka, R.; Juska, G. *Phys. Rev. B* **2005**, *72*, 035217.
(80) Dennler, G.; Mozer, A. J.; Juska, G.; Pivrikas, A.; Österbacka, R.; Fuchsbauer, A.; Saricifti, N. S. *Org. Electron.* **2006**, *7*, 229.
(81) Juska, G.; Sliauzys, G.; Genevicius, K.; Arlauskas, K.; Pivrikas, A.; Scharber, M.; Dennler, G.; Sariciftci, N. S.; Österbacka, R. *Phys. Rev. B* **2006**, *74*, 115314.
(82) Pivrikas, A.; Juska, G.; Mozer, A. J.; Scharber, M.; Arlauskas, K.; Sariciftci, N. S.; Stubb, H.; Österbacka, R. *Phys. Rev. Lett.* **2005**, *94*, 176806.
(83) Shuttle, C. G.; O'Regan, B.; Ballantyne, A. M.; Nelson, J.; Bradley, D. D. C.; de Mello, J.; Durrant, J. R. *Appl. Phys. Lett.* **2008**, *92*, 093311.
(84) Garcia-Belmonte, G.; Munar, A.; Barea, E. M.; Bisquert, J.; Ugarte, I.; Pacios, R. *Org. Electron.* **2008**, *9*, 847.
(85) García-Cañadas, J.; Fabregat-Santiago, F.; Bolink, H.; Palomares, E.; Garcia-Belmonte, G.; Bisquert, J. *Synth. Met.* **2006**, *156*, 944.

JP9037649